Importance of tie molecules in preventing polyethylene fracture under long-term loading conditions

A. Lustiger and R. L. Markham
Battelle-Columbus Laboratories, 505 King Avenue, Columbus, Ohio 43201, USA
(Received 28 January 1982; revised 11 April 1983)

Brittle-type slow crack fracture is the dominant mode of failure in polyethylene pipe used for natural gas distribution. Constant tensile load testing of polyethylene pipe sections indicates a link between this mode of failure and environmental stress cracking. Interlamellar fracture can occur in both the presence and absence of an accelerating environment. The fibre deformation process is reviewed, describing the role of amorphous entangled tie molecules in preventing slow crack-type fracture. Relative resistance to slow crack brittle failure is explained in terms of this model for various materials tested.

Keywords Tie molecules; polyethylene; lamellae; fracture; environmental stress cracking; pipe

INTRODUCTION

The term 'brittle failure' is applied to fracture accompanied by relatively little deformation or material flow in the crack area. Impact loading often results in brittle failure. Preventing this type of brittle fracture through proper design is a prime concern for manufacturers and users of plastic, especially of glassy polymers such as polystyrene and polymethyl methacrylate.

Recently, however, a different type of brittle behaviour in polyethylene, associated with long-term, low-level loading conditions, has been reported. In contrast to instantaneous impact-type fracture, failures of this type usually occur over a relatively long period of time, and are characterized by a slow crack growth. This brittle behaviour differs from the ductile, creep-type behaviour previously thought to be the only failure mechanism occurring in polyethylene under long-term, low-level stresses.

A similar type of brittle failure, environmental stress cracking (ESC), occurs when polyethylene is subjected to stress in the presence of various detergents and alcohols. ESC has been the subject of many publications since it was first observed in the early 1950s[1]. In view of recent experience with the intrinsic brittle failure of polyethylene in the absence of any accelerating environment, it may be worthwhile to explore on a molecular level the link between this type of fracture and ESC.

In the case of polyethylene piping used in natural gas distribution, the implications of this brittle-type failure are a major concern. As a result, the work described here was carried out directly on extruded, medium-density polyethylene pipe to examine the practical aspects of this phenomenon, to describe a model for brittle fracture and to rationalize property differences on this basis.

EXPERIMENTAL

The medium-density polyethylene pipes studied were 25.4 mm in diameter and met the PE2306 and PE3406 Plastics Pipe Institute standards designation[2]. The codes following the PE2306 or PE3406 designation identify the manufacturer, the extruder, and the date of extrusion through the roman numeral, the letter, and the subsequent three or four digit number, respectively.

In the constant tensile load test, a ring 12.7 mm wide is cut from the pipe. The ring is axially notched on both the inside and outside walls to a depth of 1.5 mm at the region of minimum wall thickness and at 180° from this point. The ring is then placed in a split-ring fixture and placed under a constant load in either the presence or absence of a 1% solution of Igepal CO-630* surfactant in water at 23°C. A specimen mounted in the constant tensile load test fixture is shown in *Figure 1*. After failure, specimens were examined using the scanning electron microscope (SEM).

To elucidate the brittle failure mechanism, environmental stress cracks were initiated on the inside surface of a spherulitic pipe by flattening a ring cut from the pipe and then placing the ring in a fixture in 25% Igepal solution at 50°C. The complete procedure, known as the Compressed Ring Test, is described in a previous paper[3]. The ring specimen, which displayed widespread microcracking on the inside surface after testing, was then etched using the permanganate technique of Bassett and Olley[4]. A portion of this specimen was examined using the SEM and then replicated for examination using the transmission electron microscope (TEM). Subsequent morphological examinations of the inside pipe wall were carried out on a number of the pipes studied using the same etching technique. Gel permeation chromatography (g.p.c.) and a density gradient column were used to measure molecular weight distribution and density differences between selected piping materials.

RESULTS AND DISCUSSION

Constant tensile load data

Constant tensile load data obtained on 25.4 mm diameter polyethylene pipe in both Igepal and air are shown

---

* GAF Corporation, 1424 W. 51st Street, New York, NY 10020, USA

0032-3861/83/121647-08$03.00

in *Figures 2* and *3*. The ordinate of each plot is labelled 'reduced stress', defined as the percentage of applied or nominal stress to yield stress. The usefulness of this parameter is explained later.

Figure 2 is a plot of reduced stress *versus* failure time data for seven different lots of polyethylene piping materials in Igepal. The curve that is generated typically has a shallow-sloped region followed by a more steeply sloped region. Generally, ductile-type failure showing large deformation and necking, corresponding to relatively high stress levels and short failure times, occurs in the shallow-sloped region of the curve. In the region of lower stress levels and longer failure times, a brittle-type failure occurs, characterized by little deformation at the point of failure and corresponding to the region of the curve where the slope is steeper. The point where the slope changes can be characterized as a type of 'ductile–brittle transition', although prior use of this term generally has been limited to impact fracture.

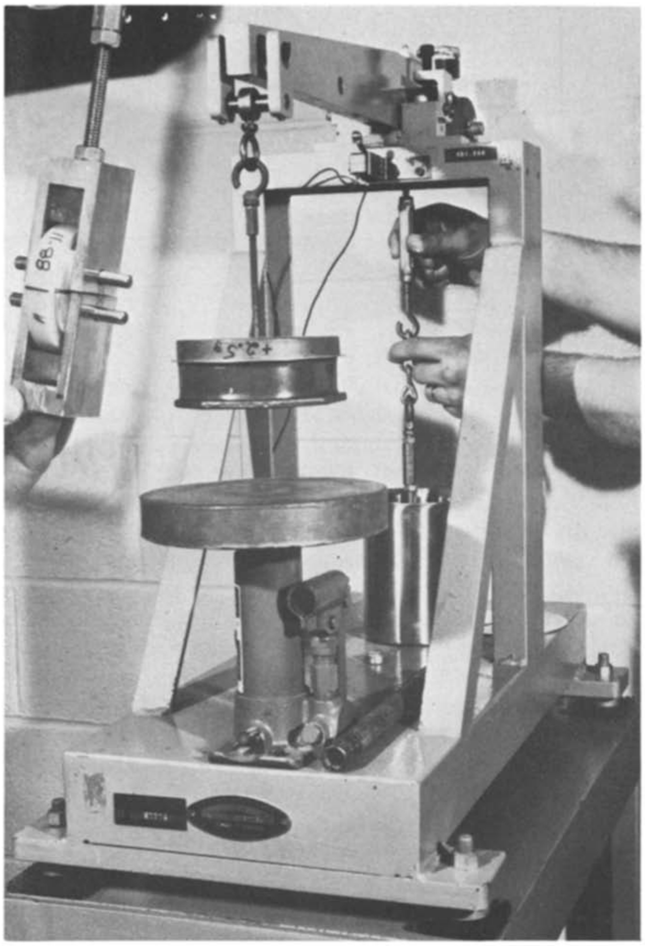

Figure 1 Test fixture and specimen configuration (inset) for the constant tensile load test

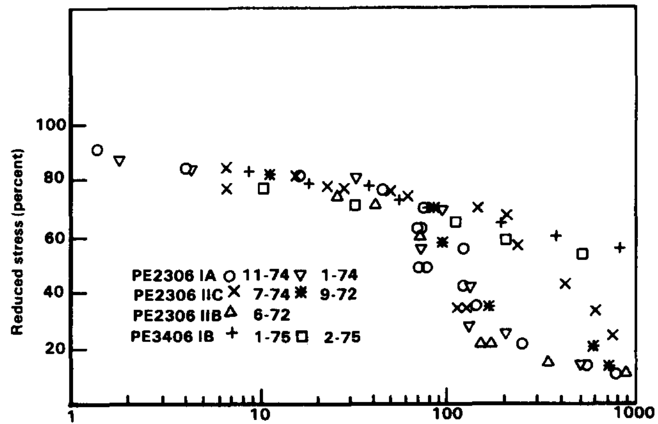

Figure 2 Reduced stress *versus* failure time for seven polyethylene materials in Igepal

Comparing different medium-density polyethylene materials with differing yield points results in a wide band of scattered data in the ductile portion of the curve when the ordinate is labelled 'nominal stress' rather than 'reduced stress' (*Figures 4* and *5*). Dividing applied stress by the yield stress for all pipes tested thus tends to normalize the data in the ductile region of the curve. *Table 1*, which describes the linear correlation factors in the ductile region for both sets of data, shows that this normalization is statistically significant.

Analysing and contrasting the curves in *Figures 2* and *3* indicates the utility of ESC resistance testing for evaluating polyethylene pipe.

For the materials labelled PE2306IA-1174, PE2306IA-174, PE2306IIC-972, and PE2306IIB-672, a ductile–brittle transition occurs at approximately 70 h in Igepal, while the same materials in air have a transition at approximately 160 h. For the PE2306IIC-774 material,

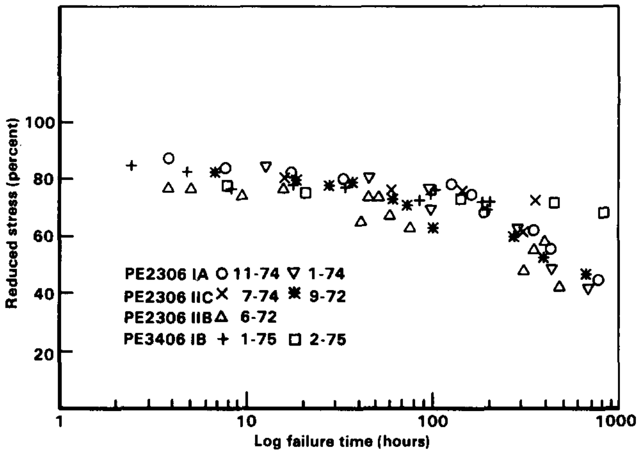

Figure 3 Reduced stress *versus* failure time for seven polyethylene materials in air

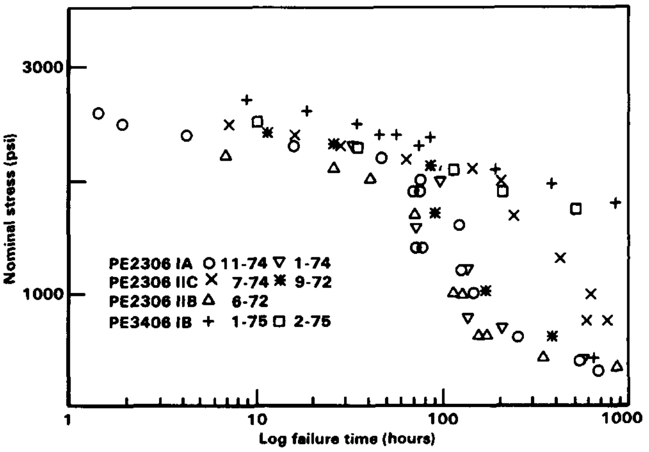

Figure 4 Nominal stress *versus* failure time for seven polyethylene materials in Igepal

however, the transition in Igepal occurs at 200 h with no apparent transition in air during the 1000 h that the material was on test. In view of the results of the four materials described previously (PE2306IA-1174, PE2306IA-174, PE2306IIC-972, and PE2306IIB-672), it is expected that a transition in air would in all probability have taken place in the PE2306IIC-774 material had the specimens remained on test after 1000 h. Similarly, for the two PE3406IB materials tested, which display no transition in air or in Igepal, longer testing would probably have revealed a ductile–brittle transition.

Microscopic examination

The distinction between a 'ductile' and 'brittle' failure is not merely one of convention. The respective fracture surfaces clearly show a fibrous surface in the ductile failure as opposed to a surface which macroscopically appears smooth in the brittle failure (*Figures 6* and *7*). The SEM micrographs, *Figures 8a* and *8b*, show uniform fibre pullout in the ductile failure fracture surface, while *Figures 9a* and *9b* show the much shorter isolated fibre structure characteristic of brittle failure.

To observe the initiation process for environmentally enhanced brittle failure in more detail, widespread cracks were induced on the inside surface of a spherulitic pipe using the compressed ring procedure. This sample was etched and then examined using the SEM, *Figure 10*. The permanganate etching technique clearly reveals the spherulitic rings, although it also apparently leaves fine bumpy textured artefacts on the surface. An environmental stress crack can be seen traversing the Figure. Close observation of this crack indicates that its preferential path is either directly down the centre of the spherulites or between them, which supports the supposition that ESC is an interlamellar failure process. The region designated 'A' is apparently the one exception, with cracking being observed obliquely splitting one specific spherulite. The mechanics in this latter case were evidently not favourable for interlamellar failure as the crack would have to deviate greatly to traverse either a spherulite boundary or spherulite nucleus. Similar interspherulitic and intraspherulitic environmental stress crack initiation in films of high-density polyethylene has been reported[5].

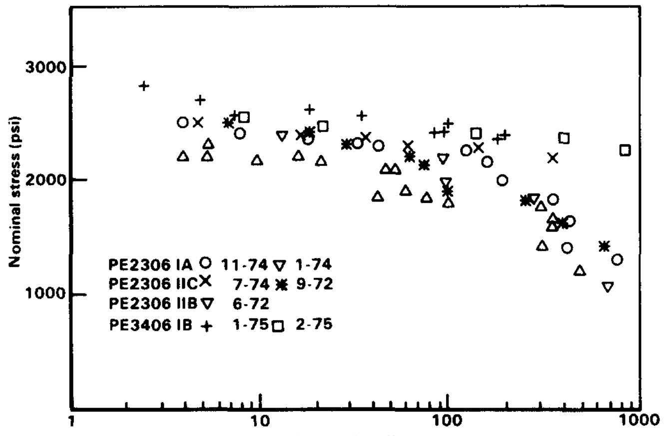

Figure 5 Nominal stress *versus* failure time for seven polyethylene materials in air

Table 1 Linear correlation factors for data in ductile regions of *Figures 2–5*

	Stress *versus* failure time	Reduced stress *versus* failure time
Igepal (36 data points)	−0.838	−0.940
Air (50 data points)	−0.592	−0.790

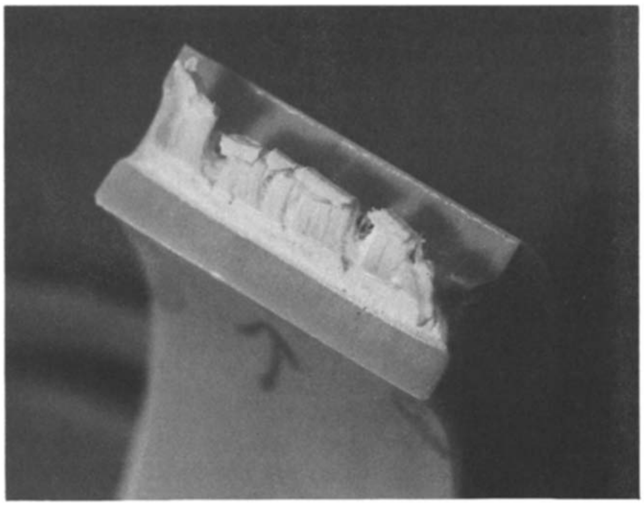

Figure 6 Fracture surface after ductile failure

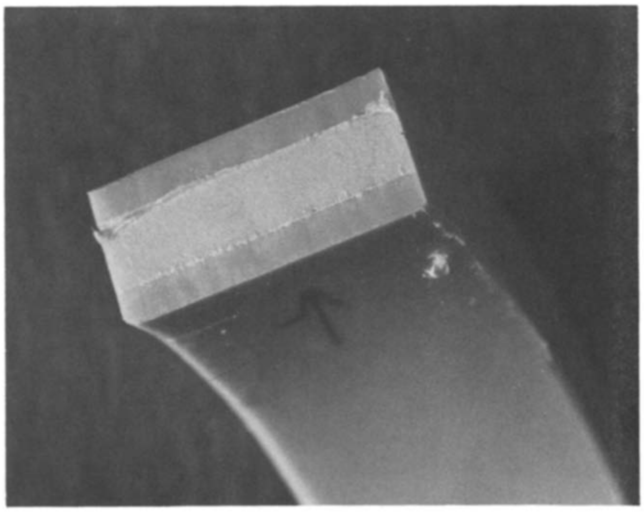

Figure 7 Fracture surface after brittle failure

Using TEM, the spherulitic rings and the orientation of lamellae can be clearly resolved (*Figure 11*). A microcrack between lamellae is apparent at higher magnification (*Figure 12*). This separation process is presumably the cause of initiation of environmental brittle fracture. A similar phenomenon has been reported for intrinsic brittle fracture in air[6].

A graphic model for failure

All these data imply that intrinsic brittle fracture under long-term low-level loading conditions is apparently related to environmental stress cracking in Igepal. To describe this behaviour on a molecular level and help visualize which structural variables most directly influence the cracking, it is worthwhile to review the fibre deformation process in semicrystalline polymers through

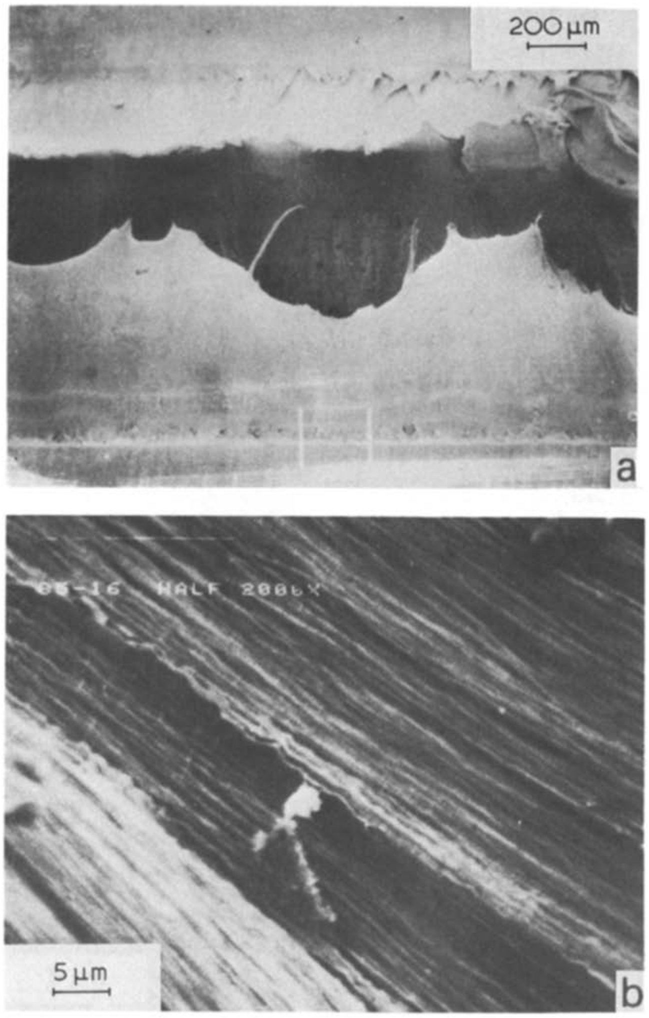

Figure 8 SEM micrographs of fracture surface after ductile failure

a model which can then be used to contrast ductile behaviour with the brittle behaviour generally observed at lower loading levels in polyethylene.

Molecular elements. Although some controversy still exists concerning the exact conformation of polymer chains in lamellae[7,8], it is assumed for purposes of this model that these chains fold on each other.

In an examination of the failure mechanism it is important to consider the intercrystalline or amorphous polymer chains. *Figure 13a* is a simplified schematic diagram showing three types of intercrystalline material: (1) cilia—chains suspended from the end of a crystalline chain; (2) loose loops—chains which begin and end in the same lamella; and (3) tie molecules—chains which begin and end in adjacent lamellae.

Ductile deformation. If a tensile load is applied normal to the face of the lamellae, the tie molecules stretch as shown in *Figure 13b*. (Note that in the model the tie molecules are illustrated as continuous chains traversing adjacent lamellae, although in reality they consist of many entanglements.) At a certain point, however, they can be pulled out no further (*Figure 13c*). At this time, the lamellae break up into smaller units (*Figure 14a*). According to this model, as advanced by Peterlin[9], these so-called 'mosaic blocks' are directly incorporated into a new fibre morphology (*Figure 14b*).

For semicrystalline polymers this model of ductile fibre pullout and, by implication, of creep deformation is far from being universally accepted. For example, Corneliussen and Peterlin[10] have shown, using small-angle X-ray scattering, that the fold period of chains in lamellae is usually different from the period of folded chains in the fibres. This finding suggests that the direct incorporation of mosaic blocks into fibres may be a misleading notion. Others suggest that in the ductile deformation of semicrystalline polymers, folded chains actually unfold as a

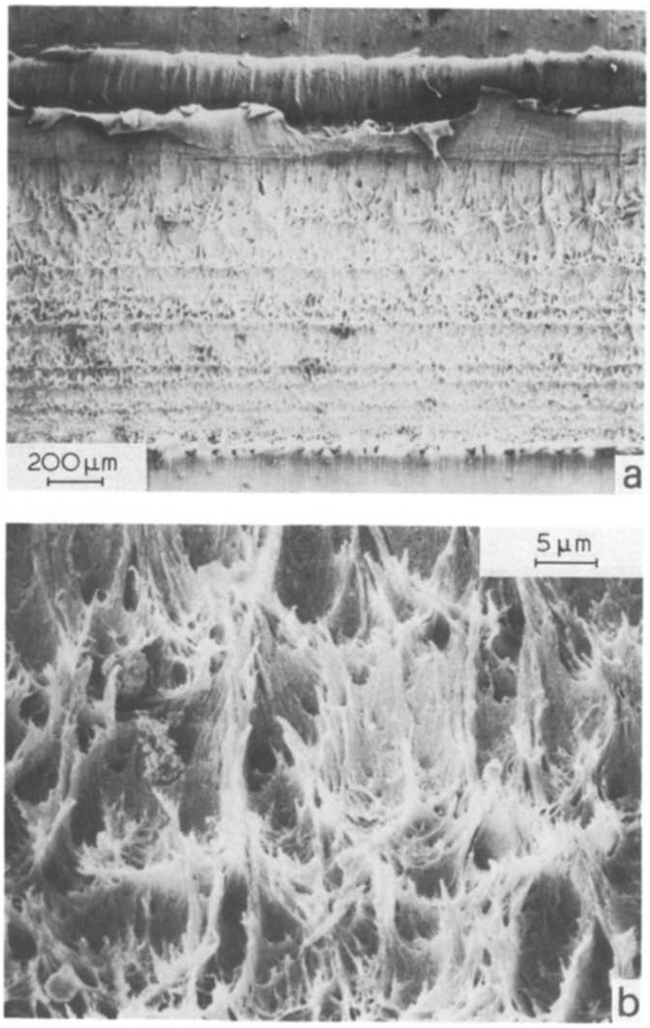

Figure 9 SEM micrographs of fracture surface after brittle failure

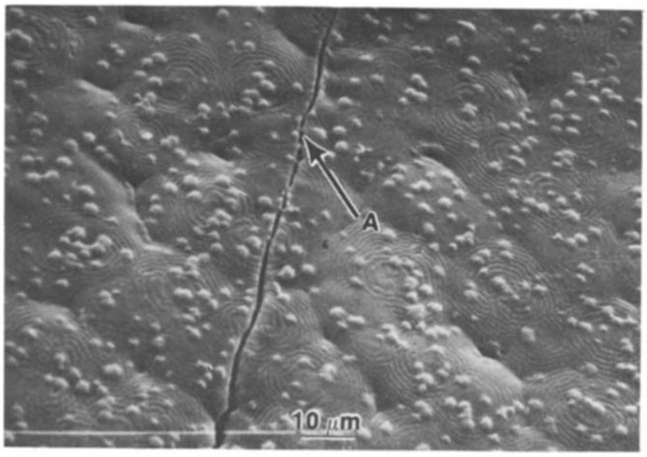

Figure 10 SEM micrograph of ESC path in spherulitic pipe

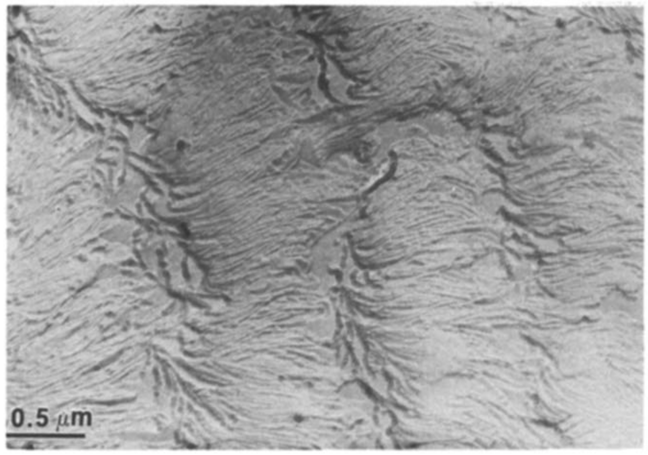

Figure 11 TEM micrograph at low magnification of portion of spherulite in spherulitic pipe after undergoing ESC

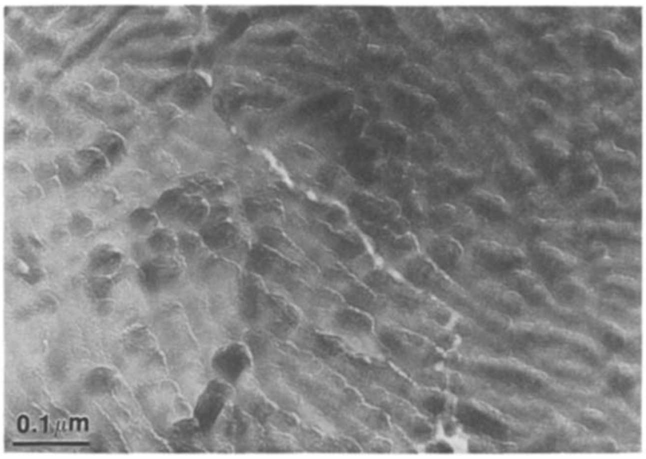

Figure 12 TEM micrograph at high magnification of portion of spherulite in spherulitic pipe showing lamellar separation

result of the force of the tensile stress[11], or undergo a stress-induced phase change[12] and renucleate into the fibres shown in *Figure 14b*. Whichever model is more accurate, the important point of this analysis is the role of tie molecules in ductile deformation. As tie molecules essentially are the 'cement' holding the lamellar 'bricks' together, their integrity is critical for ductile-type behaviour to occur.

Brittle failure. Brittle-type slow crack behaviour occurs over longer periods of time at lower stress levels than the ductile deformation discussed previously. The first three steps in this process are similar to those illustrated in *Figure 13*. However, the stress necessary to achieve large scale fibre pullout is not attained because the material is under a lower stress level. Therefore, the loading situation can be expected to remain as shown in *Figure 13c* for a relatively long time, although under long-term low-level stress, tie molecules can begin to untangle and relax. After a finite period of time most of the tie molecules untangle so that ultimately the load cannot be supported by the few tie molecules remaining and as a result the material fails in a brittle manner. Thus, the material passes from the state in *Figure 13* to that of *Figure 15*.

From the constant tensile load data, it appears that the Igepal solution accelerates the brittle failure process. The molecular displacement associated with brittle failure seems to be enhanced in the presence of Igepal. Presumably, brittle failure in polyethylene is an intrinsic phenomenon, an effect that is merely accelerated by the presence of Igepal. Interlamellar failure, which is the proposed rationale for ESC in general[13,14] can be seen as a rate-dependent process; i.e., given sufficient time at stresses below those resulting in ductile failure, tie mole-

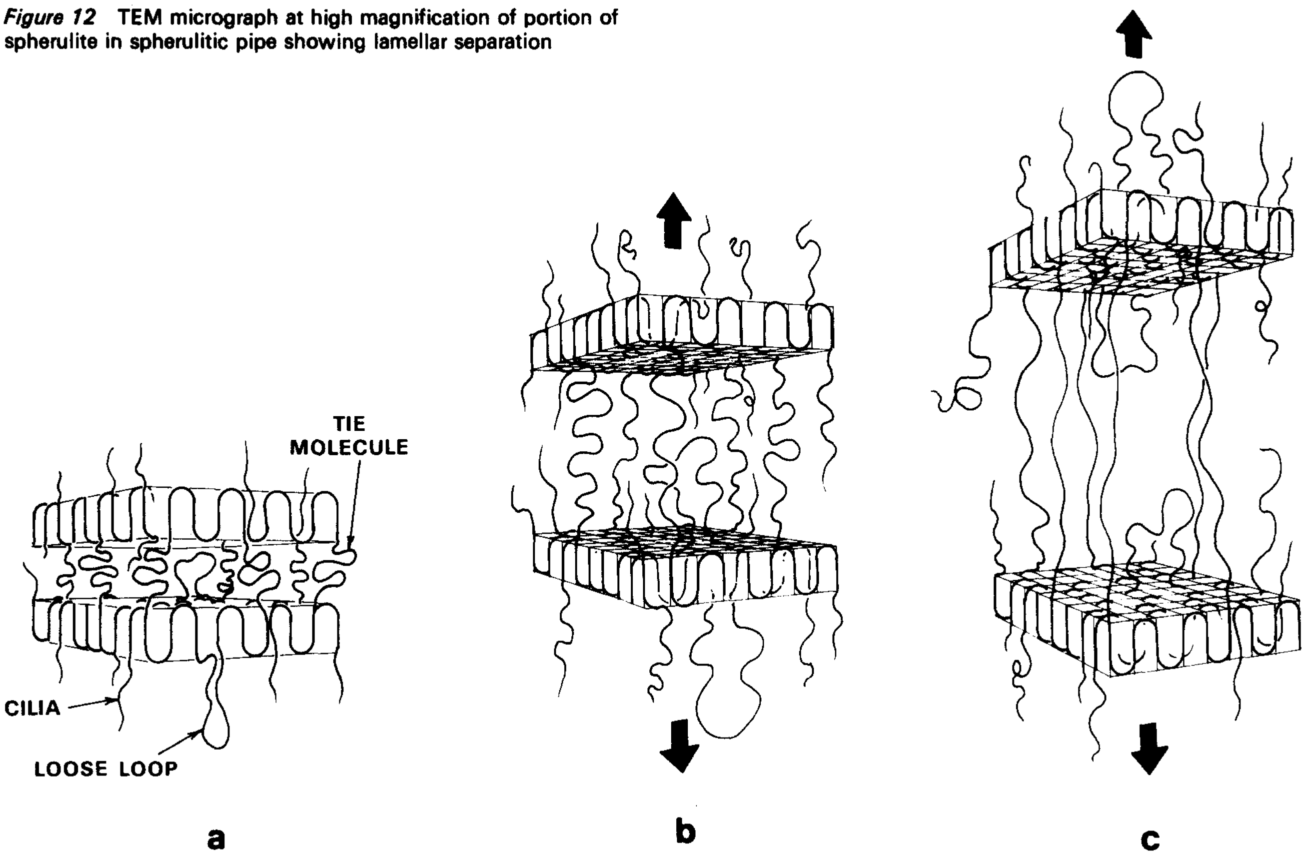

Figure 13 Initial steps in the deformation of polyethylene

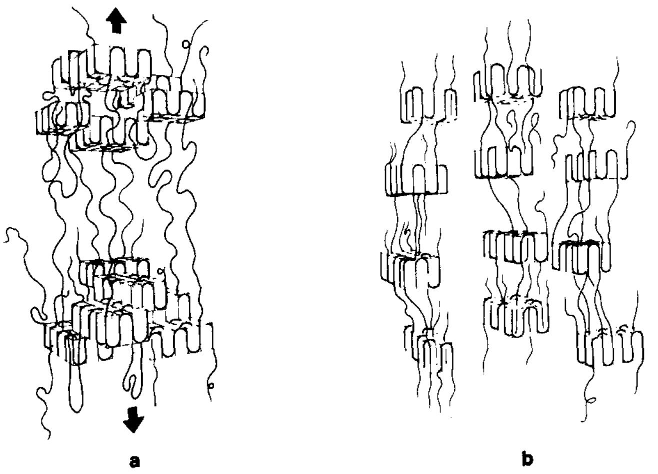

Figure 14 Steps in the ductile (creep) deformation of polyethylene

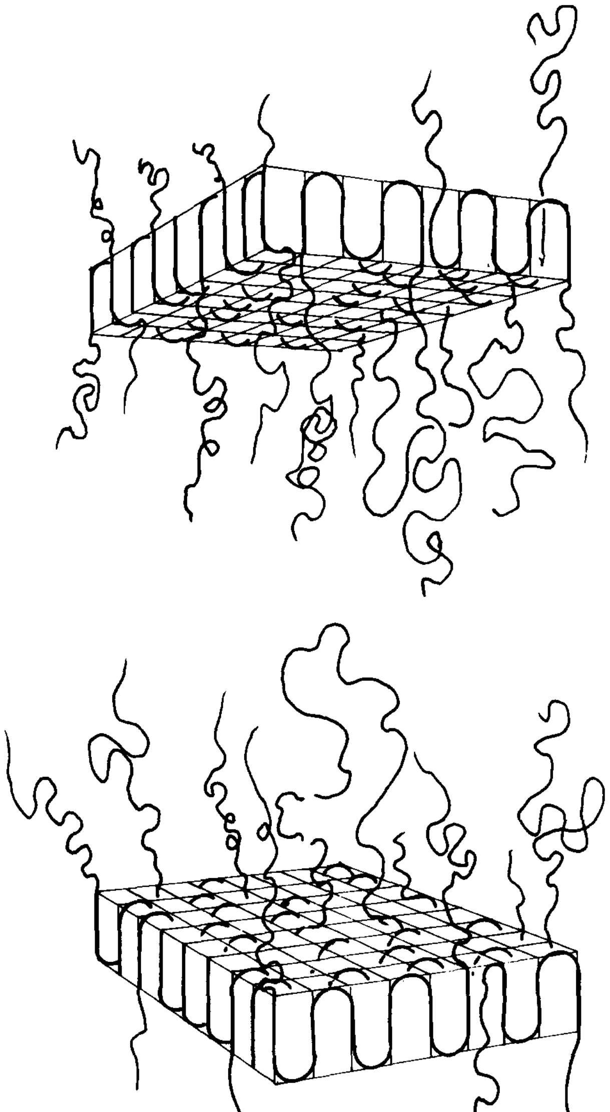

Figure 15 Final step in the brittle failure of polyethylene

cule entanglements will relax, resulting in brittle failure without any environment to 'lubricate' the tie molecules, although the failure will be accelerated in the presence of such a 'lubricant' or plasticizer. The plasticization of tie molecules has previously been ascribed specifically as the ESC mechanism[15-17].

Thus, the short non-uniform fibre formation observed for brittle failure in *Figures 9a* and *9b* is caused by an interference in the fibre formation process occurring as a result of interlamellar failure.

Important structural parameters

It follows from this discussion that polyethylene materials containing relatively few tie molecules are more susceptible to the various brittle modes of failure. Conversely, materials with relatively high concentrations of tie molecules are more resistant to these types of failures.

However, it should be added that if the proportion of tie molecules to crystalline molecules is too high, the material will display high ductility, but also very low stiffness. As, in the case of polyethylene pipe, the material must have a certain stiffness to resist exterior mechanical deformation, a balance must be established. As a result, medium-density polyethylenes are generally used in this application rather than high- or low-density polyethylenes.

Visualizing the mechanism of brittle failure in terms of the model can help identify molecular parameters of importance in optimizing piping materials for resistance to slow crack growth. Some of these parameters are:

(1) *Molecular weight.* The higher the molecular weight, the longer the polymer chains, resulting in more tie molecules and more effective tie molecule entanglements. As polymers are polydisperse, the entire weight distribution is a critical factor[18].

(2) *Comonomer content.* Because of a small amount of comonomer such as 1-butene or 1-hexene, medium-density polyethylenes contain short branches which tend to inhibit crystallinity. Higher comonomer concentration and longer comonomer short-chain branches provide better brittle fracture resistance, because the portions of polymer chains with the longer branches (i.e. 1-hexene or longer) probably do not enter the tightly packed lamellar lattice and hence add to the intercrystalline tie molecule material[17]. Another possible effect of short-chain branching is the increased effectiveness of tie molecule entanglements because the chain in effect contains protrusions, thereby inhibiting the ability of the tie molecules to slip past one another.

(3) *Density/degree of crystallinity.* It would be expected that the more crystalline the material, the fewer amorphous intercrystalline tie molecules hold it together.

(4) *Lamellar orientation.* If the lamellae are preferentially oriented perpendicular to the tensile stress direction, they would be more amenable to interlamellar failure than if they are parallel to the stress. For a spherulitic polyethylene, this effect would be minimized because in spherulites the lamellae are oriented radially. (Examples of apparently nonspherulitic polyethylene are described later.)

Rationalizing property differences

The data in *Figure 2* indicated significant property differences among the seven pipes tested. Many of these differences can be rationalized based on the important structural parameters identified previously. This discussion considers property differences in four of the seven pipes tested under constant tensile load as shown in *Figure 2*:

(1)PE2306IA-1174 (Ductile–brittle transition in Igepal, 70 h).

(2) PE2306IIC-972 (Ductile–brittle transition in Igepal, 70 h).

(3) PE2306IIC-774 (Ductile–brittle transition in Igepal, 160 h).

(4) PE3406IB-275 (Ductile–brittle transition in Igepal, > 1000 h).

Three different piping materials are represented. PE2306IIC-972 and PE2306IIC-774 are two lots of the same piping material originating from the same extruder.

Density/molecular weight. Basic density and molecular weight data for these materials are given in *Table 2*. Although the density data alone would suggest that the PE3406 material would display the most brittle behaviour (i.e. an early transition) the molecular weight data for this material indicate a molecular weight distribution which would retard brittle fracture. A composite plot of molecular weight distribution curves is shown in *Figure 16* for PE2306IA-1174, PE2306IIC-774, and PE3406IB-275. These curves reveal that (1) PE2306IA-1174 has a relatively low amount of low molecular weight molecules but also the lowest fraction of high molecular weight molecules, (2) PE2306IIC-774 has a higher number of short chains but a significantly higher proportion of high molecular weight molecules, and (3) although PE3406IB-275 has relatively few low molecular weight molecules, as does PE2306IA-1174, it also contains a high molecular weight fraction even larger than that for the PE2306IIB-774.

Based on the description of the model for graphic failure, higher molecular weight will considerably delay brittle fracture because of the relatively large number of tie molecules which result. This explains the improved crack resistance of the PE3406 material as compared with the other materials.

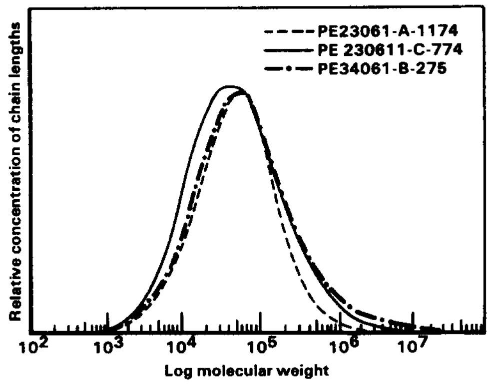

Figure 16 Composite molecular weight distribution curve for PE2306IA–1174, PE2306IIC–774, and PE3406IB–275

Morphology/comonomer content. The property differences represented by the three PE2306 materials are not as easily explained. The situation is complicated by the significant differences in the ductile–brittle transitions reflected in the two lots of the same PE2306IIC materials. *Table 2* indicates no significant density or molecular weight variations to justify the difference in 'ductile–brittle' transition between these two.

The morphology of the PE2306IA-1174 was found to be spherulitic (*Figure 17*) unlike both PE2306II materials which were found to be apparently non-spherulitic. However, a significant difference was noted in the lamellar orientation in the non-spherulitic pipes. In the PE2306IIC-774 pipe, the lamellae are randomly oriented (*Figure 18*); in contrast, the PE2306IIC-972 pipe has regions with lamellae preferentially oriented in the extrusion (axial) direction perpendicular to the pipe surface (*Figure 19*).

This preferential orientation would be expected to have a deleterious effect on brittle fracture resistance. As brittle-type slow crack fracture is interlamellar in nature, the axial orientation of lamellae and the specimen orientation in the constant tensile load test, which induces failure in the axial direction, would render the PE2306IIC-972 material more susceptible to brittle failure. These subtle differences in morphology may explain the perceived property differences between the two PE2306II materials, despite the fact that the resin, coming from the same manufacturer, is at least nominally the same. It is

Figure 17 TEM micrograph of spherulitic PE2306IA–1174 after permanganate etching

Table 2 Density and molecular weight distribution data for four PE piping materials

	PE2306IA–1174	PE2306IIC–972	PE2306IIC–774	PE3406IB–275
Density (g cm^{-3})	0.9406	0.9406	0.9393	0.9514
Molecular weight data				
$M_w \times 10^{-4}$	10.65	11.55	12.79	27.5
$M_n \times 10^{-4}$	2.43	1.44	1.53	2.72
$M_z \times 10^{-4}$	61.02	80.67	88.44	288.4
$M_{z+1} \times 10^{-4}$	207.9	223.9	227.4	702.7
M_w/M_n	4.4	8.2	8.4	10.0

Figure 18 TEM micrograph of apparently non-spherulitic PE2306IIC–774 showing random lamellae

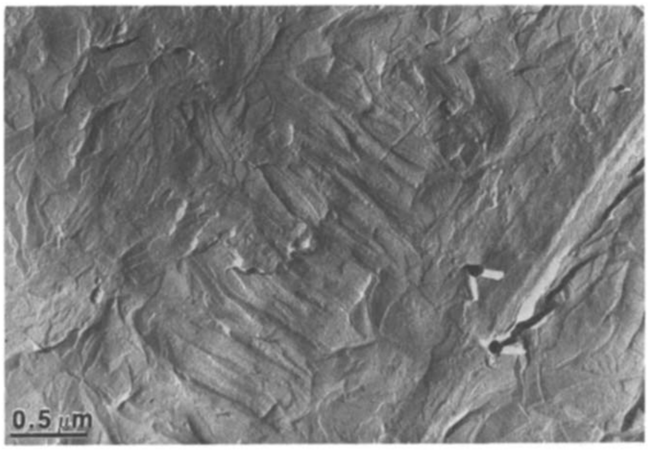

Figure 19 TEM micrograph of apparently non-spherulitic PE2306IIC–972 showing regions of preferential orientation of lamellae

probable that these differences are related to extrusion conditions rather than basic lot-to-lot differences in polyethylene resins, although the precise extrusion conditions necessary to duplicate the oriented lamellar morphology are unknown.

However, these results should be considered with some caution. Although the non-spherulitic morphology has been well documented[19], and the absence of a small-angle light scattering pattern in the PE2306II materials seems to confirm its non-spherulitic nature, it has been shown recently that the inside surface of polyethylene pipes can often be thermally oxidized during extrusion. This oxidation can alter the morphology of this surface[20]. As a result of this indication in the literature, the bulk morphology of the pipe cross-sections will be examined once the precise etching conditions are refined.

In addition to significant morphological differences between the PE2306IA-1174 and the two PE2306II materials, differences in molecular weight and comonomer were also documented. PE2306IA-1174 displayed an average spherulite size of 22 μm diam., as well as relatively low weight average and z-average molecular weights. PE2306IA-1174 was found to contain the shorter 1-butene chains as opposed to the 1-hexene chains of the PE2306II materials. Apparently, the combined effect of morphology, molecular weight, and comonomer differences contribute to the relatively early ductile–brittle transition in the PE2306I material.

CONCLUSION

Environmental stress cracking in polyethylene is apparently an acceleration of the brittle-type slow crack failure process which would intrinsically occur in air at a later time under similar test conditions. The relaxation of tie molecules and the resulting interlamellar failure, therefore, can occur in either air or Igepal. Use of a graphic failure model can help identify which structural variables most directly influence this property. These have been shown to include degree of crystallinity, molecular weight distribution, branch length, and lamellar orientation.

ACKNOWLEDGEMENT

The authors would like to thank the Gas Research Institute for sponsoring this research under Contracts 5014-352-152 and 5082-260-0613. The authors are also indebted to colleagues Michael J. Cassidy, Larry A. Smith and Andrew Skidmore for their technical help, and to Professor Roger D. Cornelivssen of Drexel University for helpful discussion.

The Gas Research Institute makes no warranty as to the accuracy or completeness of this report and assumes no liability for the use of information disclosed in it.

REFERENCES

1 Howard, J. B. *SPE J.* 1959, **6**, 397
2 ASTM Standard D3350-78 (1982 Book of ASTM Standards), Part 34
3 Lustiger, A., Markham, R. L. and Epstein, M. M. *J. Appl. Polym. Sci.* 1981, **26**, 1049
4 Olley, R. H., Hodge, A. M. and Bassett, D. C. *J. Polym. Sci. A-2* 1979, **17**, 627
5 Haas, T. W. and MacRae, P. H. *SPE J.* 1968, **24**, 27
6 Petermann, J. and Schultz, J. M. *J. Mater. Sci.* 1978, **13**, 50
7 Yoon, D. Y. and Flory, P. *Polymer* 1977, **18**, 509
8 DiMarzio, E. A. and Guttmann, C. M. *Polymer* 1980, **21**, 118
9 Peterlin, A. *J. Macromol. Sci. Phys.* 1973, **B8**, 83
10 Corneliussen, R. and Peterlin, A. *Makromol. Chem.* 1967, **105**, 193
11 Gleiter, H., Horbogen, E. and Petermann, J., Battelle Institute Seventh Materials Science Colloquium, Plenum, N.Y., 1973, pp. 149–169
12 Juska, T. and Harrison, I. R. *Polym. Eng. Revs.* 1982, **2**, 13
13 Bandyopadhyay, S. and Brown, H. R. *Polymer* 1978, **19**, 589
14 Singleton, C. J., Roche, E. and Geil, P. H. *J. Appl. Polym. Sci.* 1977, **17**, 27
15 Frayer, P. D., Tong, P. P. L. and Dreher, W. W. *Polym. Eng. Sci.* 1977, **17**, 27
16 Hannon, J. M. *J. Appl. Polym. Sci.* 1974, **18**, 3761
17 Brown, H. R. *Polymer* 1978, **19**, 1186
18 Herman, J. N. and Biesenberger, J. A. *Polym. Eng. Sci.* 1966, **6**, 341
19 Mandelkern, L., Glotin, M. and Benson, R. A. *Macromolecules* 1981, **14**, 34
20 Terselius, B., Gedde, U. W. and Jansson, J. F. *Polym. Eng. Sci.* 1982, **22**, 424